International Journal of Advanced Technology and Engineering Exploration, Vol 10(104)
ISSN (Print): 2394-5443 ISSN (Online): 2394-7454
http://dx.doi.org/10.19101/IJATEE.2022.10100477

Research Article

Gain enhancement of a monopole antenna using frequency selective surface for sub-6 GHz band applications

Shabnam Ara* **and Prasanthi Kumari Nunna**
Department of Electronics and Communication Engineering, School of Engineering and Technology, University of Petroleum and Energy Studies, Dehradun (Uttarakhand), India

Received: 29-November-2022; Revised: 05-July-2023; Accepted: 08-July-2023

Abstract
A monopole edge-fed triple-layered double-story rectangular patch antenna was designed in this study. The antenna was loaded with a frequency selective surface (FSS) to enhance its gain and radiation efficiency. Several antennas were designed without the reflector, and in this proposed work, an FSS was placed beneath the reduced length ground plane to act as a partial reflector for the antenna's back lobes. The microstrip rectangular patch antenna with an inset feed was fabricated on a low-loss RT Duroid 5880 substrate measuring 49mm × 49mm × 1.588mm. The FSS, on the other hand, was fabricated on an FR4 substrate of the same size. The FSS consisted of an array of equally spaced 49 rectangular dipole strips. When comparing the antenna with and without the FSS, it was found that the antenna without the FSS had a gain of 2.87dBi and a -10dB fractional bandwidth (FBW) of 92.66%. However, the antenna with the introduced FSS demonstrated an improved gain of 7.76dBi (an enhancement of 4.91dBi) and a reduced -10dB FBW of 49.08%. The introduction of the FSS resulted in improved radiation characteristics, transforming the bi-directional radiation pattern into a unidirectional one, and significantly improving the front-to-back ratio (FBR). Furthermore, the radiation efficiency of the antenna without the FSS at its resonant frequency of 5.8GHz was measured to be 94.68%, while with the FSS reflecting surface, it increased to 97.88%. The antenna with the FSS achieved a reflection coefficient below -10dB over a wideband range from 3.90GHz to 6.43GHz. Consequently, the proposed antenna was deemed suitable for various applications, including 5.8GHz WLAN and 5G sub-6 GHz bands such as n46 (5150 – 5925MHz), n47 (5855 – 5925MHz), n77 (3900-4200MHz), n79 (4400-5000MHz), and n96/n102 (5925-6425MHz). Additionally, this study presented the electrical equivalent, resistive inductive capacitive (RLC) circuit of the proposed antenna.

Keywords
Dipoles, Frequency selective surface (FSS), Gain, Microstrip patch antenna (MPA), Wideband (WB).

1.Introduction
The development of wireless communication technology has increased the demand for research and antenna structure designs. As compared to traditional antennas, microstrip patch antennas (MPA) have made great progress in the field of research owing to their affordability, low profile, lightweight design, and ease of fabrication. The substrate and its physical properties play a major role in the antenna's performance. A MPA has a design similar to a sandwich, in which the main patch is on top, a substrate in the middle, and the ground plane at the bottom. The Wi-MAX, Wi-Fi, mobile communication, and internet of things (IoT) applications are emerging in the recent past drastically. That necessitates the requirement of low-profile, affordable, and mechanically durable antennas. Those can be mountable on unyielding planes. Undoubtedly, MPA were always the first choice of antenna engineers in such applications [1–3]. Multiple design methods for MPA have already been available in the literature, whose objectives are to the enhancement of complete attainment parameters e.g. reflection coefficient, bandwidth, radiation efficiency, and antenna gain. Despite having many benefits, microstrip antennas have numerous limitations, such as low efficiency, spurious feed radiation, lower power, high Q, and extremely limited bandwidths [4, 5]. However, for the past decade, several researchers and antenna designers are working on increasing the patch antenna's gain. The higher gain has a beneficial footprint on network applications. High gains are being used to fulfill

*Author for correspondence

these objectives based on fifth generation (5G) applications and various features. Due to the wide variety of applications, there is an increasing need for high-gain antennas that can function in 5G frequency ranges. Antennas wihout frequency selective surfaces (FSS) have bidirectional radiation patterns, limited gain, lower Front to back ratio, and lower radiation efficiencies [6].

To filling the research gap and to achieve high-gain performances, a variety of techniques have been suggested like the array of metamaterial especially split ring resonators (SRRs), resistive interface surface (RIS), fractal structure, electromagnetic band gap (EBG), superstrate and FSS [7]. A frequency-selective surface is one utilizing technique, which uses periodic patterns in the structure to create reflection and transmission behavior. So far several methods have been recommended and applied to improve the performance parameter of MPA [8, 9]. High gain and directional pattern antenna is the base for microstrip line to waveguide transitions [10–12]. These antennas play the role of launching elements [13–15]. The following are the main objectives of this proposed research;

-The primary objective of the proposed antenna using FSS is to design a compact antenna and enhance the antenna gain and other performance parameters. Flexibility and ease to manufacture are important factors.

-Another objective of the research is to observe the parametric effect of antenna parameters and FSS structure optimization to obtain the required frequency band for 5G sub-6 GHz applications [16].
-Furthermore, the final objective of this work is to obtain the unidirectional radiation pattern by placing an FSS below the patch antenna on a low-profile FR-4 substrate to reduce the cost and improve the front-to-back ratio (FBR) and radiation and directive characteristics in one direction.

In this paper, a method is presented to obtain an enhanced high-gain monopole antenna supported by a dipole FSS reflector for sub6-GHz and 5G demands. The dipole FSS surface is made by placing the dipoles having the same width as the patch antenna substrate to boost gain at the ideal spacing discovered using the optometric tool in ANSYS High-frequency structure simulator (HFSS). Other parameters such as the width of the ground plane, spacing between the dipoles in FSS, and the width of dipoles in FSS are also obtained with the help of the Optometric tool in ANSYS HFSS.

The paper is arranged in this manner: In section-2 elaborated on the literature review, section-3 discusses the methodology of designing FSS and patch antenna are discussed and section-4 describes the simulation results analysis in detail for the cases with and without FSS is presented to justify the proposed method. Section-5 describes the study and a comparison of the simulation results of the patch antenna with a similar existing antenna and the limitations of the proposed design. Section-6 presents the conclusion and future scope of the proposed design.

2.Literature review

Many experts have employed metamaterials to construct dual band, high gain patch antennas using defective ground surface (DGS) and SRR triplet layer at the ground plane [7]. Nakmouche and Nassim [17] have designed a dual-band planar inverted - F antenna (PIFA). By utilizing fishnet-shaped metamaterials surface as DGS the antenna gain was increased from 3 dB to 8 dB. The simulation finding of the suggested Fishnet-based PIFA structure antenna demonstrates dual band frequency at 3.9 GHz and 5 GHz with enhancement in reflection coefficient, a slightly stronger overall good efficiency of 92.50%, a gain extended with 3.11dB compared to the conventional PIFA antenna gain. Nakmouche et al. [18] have developed a high-gain, stepless frequency selection (SFS) superstrate layer-based monopole antenna using machine learning. A backed FSS layer below 6mm distance from the main patch was placed for enhancement of gain. The method extends the gain from 3.12dBi to 8.89dBi and radiation efficiency higher than 95%. Substrate integrated waveguide (SIW) antenna and components are designed for gain enhancement and directional patterns. By utilizing both substrate-integrated waveguide and H-slotted DGS, Nakmouche et al. [18] have proposed a dual-band MPA for the application of Ku-band with impressive gains. Performance study of the work in antennas provides gain and directivity values of 7.03 dB and 7.38 dB at the center frequency of 12.67 GHz and 7.77 dB and 8.13 dB at the frequency of 14.56 GHz, respectively. Radiation efficiency measures 95.25% at 12.67 GHz and 95.60% at 14.56 GHz, respectively [19]. FSS is another attractive arrangement that extensively contributes to enhancing the antenna gain and overall effectiveness of MPA. It was created primarily to regulate the transmission and reflection properties of

an incident wave. Typically, it consists of a definite planar arrangement of regularly spaced-out unit cells on a dielectric substrate material. Munk [20] has fabricated a quarter-wave impedance transformer-fed microstrip antenna for gain enhancement at an industrial scientific and medical (ISM) band frequency of 2.4GHz by using a SIW FSS structure. A gain enhancement using SIW FSS was 4.15dBi [21]. In other words, FSS is a Periodic structure of unit cells that consists of metallic patches or space components. These have great transmission or reflection properties [22]. The literature has proposed a variety of antenna designs based on FSS to enhance gain. Kim et al. [23] have proposed a holey superstrate-based antenna. The superstrate hole radius adjustment changes the effective permittivity and enhances the electric field on the top surface of the superstrate. The gain enhancement was carried out by creating a larger in-phase electric field on the top surface of the superstrate. The fabricated antenna enhances the gain by 4.45dBi at a frequency of 5.8 GHz. Sarkhel and Bhadra [24], have proposed a method of slotted antenna gain enhancement by using an electric metasurface superstrate. Using metasurface the broadside gain is enhanced by 10.86dBi and radiation efficiency by 20.35%. Fernandes et al. [25] have developed a dual-band patch antenna for the ISM band using FSS as a reflector (with concentric quad square ring pair in one-unit cell of FSS for radiation characteristics. The antenna gain enhanced to 7.54 dBi and 6.8 dBi at 2.4 GHz and 5.8 GHz. Its limitation is a larger FSS size than the main substrate and a lower front-to-back lobe ratio. Tilak et al. [26] have presented a heart-shaped dual-band monopole antenna using an artificial magnetic conductor (AMC) for the enhancement of antenna resultant parameters and radiation characteristics. The antenna is perfect for the ISM band. The monopole antenna without an AMC array obtains a gain of 1.8 dBi and 2.21 dB at the frequency of 3.5 GHz Wi-MAX and 5.8 GHz W-LAN applications. The AMC is placed at a distance of a quarter wavelength (λ0/4) from the monopole antenna. The introduced 3 x 3 AMC structure enhances the gain of 5.86 dBi at the Wi-MAX band and 7.20dBi in the W-LAN applications band. Zhai et al. [27] have presented a dual-band, dual-polarized antenna with a circular ring slotted with an AMC surface for wireless local area network (WLAN) application. The dipoles are excited by two existing Baluns. The introduced AMC structure produces a unidirectional radiation pattern with enhanced peak gains of 7.3 dBi in the upper (5.12GHz to 5.62GHz), and 7.2 dBi in the lower frequency bands (2.36GHz to 2.76GHz). It reduces the cross-polarization and provides a stable radiation pattern. Liu et al. [28] have proposed a low-profile, dual-band, dual-polarized antenna for 5G sub-6 GHz mobile applications using an AMC reflector. The antenna consists of an AMC reflector and a pair of crossed dual-polarized bowtie dipoles. Gain enhancement is achieved by inserting trapezoidal and U- slots on the bowtie dipoles. The enhanced peak gain with the AMC reflector is 7.1dBi in the lower band (3.14-3.83GHz) and 8.2dBi in the upper band (4.40-5.02GHz). Ghosh et al. [29], have designed a coplanar wave guide (CPW) fed tri-band slotted patch antenna using AMC as a reflector for gain enhancement. The reflection phase at all the resonating frequencies is close to zero for better gain enhancement. It also reduces cross-polarization. The gain without AMC was 3.19dBi while with AMC gain becomes 7.32dBi. Chatterjee and Parui[30] have presented a gain enhancement method of a low-profile slotted multi-layered antenna using a second-order bandpass filter as an FSS superstrate. A total 4dBi gain enhancement over the entire band 5.0 GHz to 8.0 GHz has been noticed. Gharsallah et al.[31] have proposed a dielectric resonator antenna(DRA) with a metamaterial SRR superstrate surface for gain enhancement. The antenna attains a total gain of 11.15dBi. Belen et al. [32] have fabricated an antenna loaded with DRA and metamaterial SRR, FSS using three dimensional (3D) printing. This method enhances the antenna gain from 2.10 dBi to 6.60 dBi. Ram and Kumar [33], have developed a slotted grounded planar antenna using FSS as a reflector for gain improvement. The same substrate was used for both the antenna and FSS layer. The antenna achieves an ultra-wideband (UWB) frequency band from 3.2GHz to 12GHz. The antenna gain is enhanced from 3-4dBi over the band. It reduces cross-polarization. Bhattacharya et al. [34] have designed an ultrathin X-band double-layered FSS surface for gain enhancement using RT Duroid 5880 low-loss substrate. The top layer of the FSS consists of a tetra-arrow with four resistors and the bottom layer consists of a split circular configuration at the bottom layer in the unit cell. Finally, this FSS layer is applied on the dielectric resonator slotted hybrid antenna for gain enhancement and it results in a total gain improvement of 7.8dBi. Hussain et al. [35] have designed a spades-shape CPW-fed antenna for bandwidth and gain enhancement using a 5X5 square circular hybrid FSS for ultra-wide band (UWB) applications. After loading with the FSS antenna attains a peak gain of 10.5dBi while without FSS its gain was 6.5dBi. Ranga et al. [36] have used a

multioctave FSS reflector for UWB antenna at a frequency of 3GHz. The antenna gain remains constant 7.5dBi throughout the band 3GHz to 7GHz. Belen [37] has constructed a double-layered FSS for antenna performance enhancement in the ISM band at a frequency of 2.4GHz. A total 7.15dBi gain improvement is achieved. Ali et al. [38] have presented a modified rectangular patch antenna at mm-wave 24GHz using multi strips FSS superstrate which not only improves the -10dB bandwidth and gain but also controls the polarization and suppresses the cross-polarization.

Available research techniques are offered with a high-performance antenna design. The antennas illustrate above have a difficult construction, limited gain, and easy manufacturing are challenging tasks due to the complexity of the structure. Even if they are manufactured, they are not appropriate for 5G applications due to their poor gain and bandwidth. According to the available article based on slots, DGS, metamaterial, AMC, etc. antenna designing with improved gain and high bandwidth is very challenging. The designs of the simple structured antennas are employing the FSS layer below the ground plane, which enhances the overall performance parameter of the antenna.

3.Methodology

The size of the recommended antenna was optimized through simulation iterations. The patch is made of RT Duroid 5880 material with permittivity ε_r = 2.2, and the FSS structure is made on the FR4 substrate material with permittivity ε_r = 4.4. HFSS is used to simulate the antenna performance. The suggested antenna operates in the sub-6 GHz region, which covers a wide range of spectrum bands.

3.1Design approach

An antenna is designed by following these design steps:

- Choose a design frequency/band and the application of the antenna at this frequency/band.
- Choose a suitable material to construct the antenna with known properties like its permittivity and its thickness.
- Using the primary design equations evaluate the antenna's principal dimensions.
- Design and analyze the antenna using available design software for electromagnetic simulation.
- Fabricate the antenna to match the application after obtaining the suitable simulation results from the parametric analysis.
- Measure the antenna using a Vector network analyzer and anechoic chamber to test and verify the physical existence of the antenna reflection coefficient and its radiation pattern.
- Compare the fabricated antenna with the available similar literature antenna.
- Conclude.

The antenna design and fabrication methodology are illustrated in the systematic block diagram in *Figure 1*.

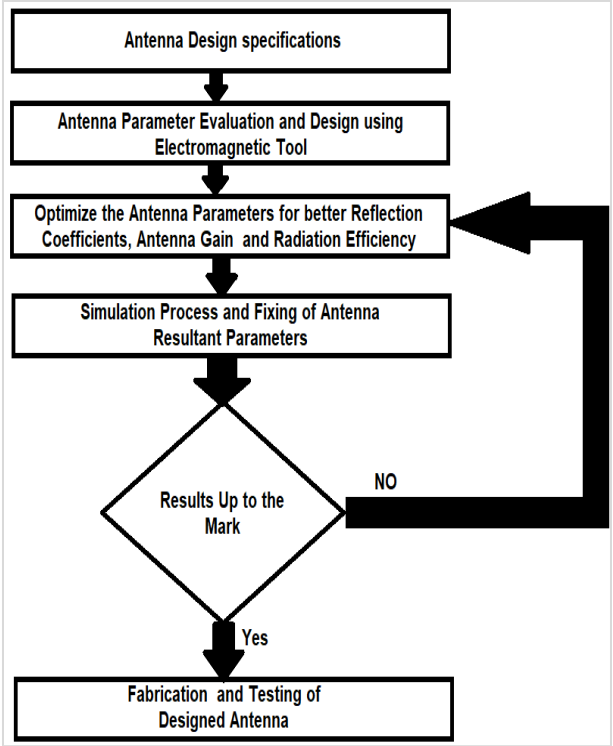

Figure 1 Block diagram of antenna design methodology

3.2Antenna geometry

The microstrip rectangular patch antenna is designed on a piece of 49 mm x 49 mm RT Duroid 5880 substrate for a design frequency f_r =5.8 GHz. The RT Duroid substrate height of 1.588mm is chosen with relative permittivity ε_r = 2.2.

3.2.1Development of rectangular patch antenna

The dimensions of the proposed microstrip rectangular patch are evaluated using Equations 1 to Equation 11 [39, 40].

The width of the patch

$$W_P = \frac{1}{2f_r\sqrt{\varepsilon_0\mu_0}}\sqrt{\frac{2}{\varepsilon_r+1}} \quad (1)$$

The effective permittivity for W/h>1

$$\varepsilon_{reff} = \frac{\varepsilon_r+1}{2} + \frac{\varepsilon_r-1}{2}\sqrt{1+\frac{12h}{W_P}} \quad (2)$$

The patch's effective length (consideration of the fringing effect).

$$\Delta L = 0.412h\frac{(\varepsilon_{reff}+0.3)(\frac{W_P}{h}+0.264)}{(\varepsilon_{reff}+0.3)(\frac{W_P}{h}+0.8)} \quad (3)$$

$$L_P = L_{eff} - 2\Delta L \quad (4)$$

Finally, we calculate the resonant frequency for the TM_{010} mode considering the fringing effect as

$$f_{r010} = \frac{c}{(2(L_P+\Delta L)\sqrt{\varepsilon_{reff}}} \quad (5)$$

Therefore, the patch length

$$L_P = \frac{c}{(2(L_P+\Delta L)\sqrt{\varepsilon_{reff}}} - 2\Delta L \quad (6)$$

50Ω Microstrip Feed Line width

$$W_f = \frac{7.48\times h}{e^{Z_0\frac{\sqrt{\varepsilon_r+1.41}}{87}}} - 1.25\times t \quad (7)$$

50Ω Microstrip Feed Line length

$$L_f = 2(\frac{\lambda_g}{4}) = \frac{c}{2f_0\sqrt{\varepsilon_{reff}}} \quad (8)$$

Substrate width

$$W_{Sub} = 3h + W_P + 3h \quad (9)$$

Substrate length

$$W_{Sub} = L_{Sub} = L_f + L_P + 3h \quad (10)$$

Ground Dimensions

$$W_{Gnd} = L_{Gnd} = W_{Sub} = L_{Sub} \quad (11)$$

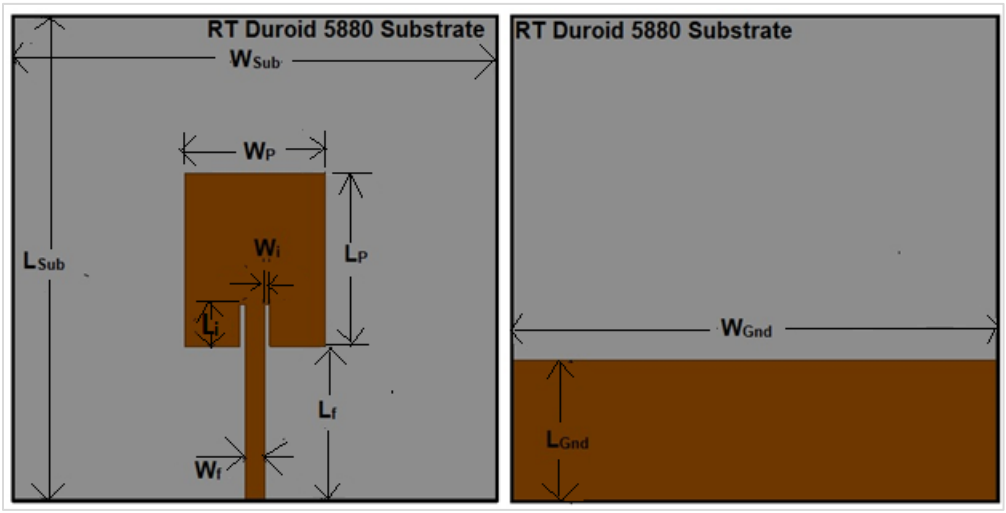

(a) (b)

Figure 2 Antenna Geometry (a) Patch side (front view), (b) Ground side (Rear View), and (c) FSS surface (dipole section)

The dimensions of the patch are calculated through the formulas available in the literature from Equation 1 to Equation 6 [7, 10, 29]. The feed width and length are evaluated using Equation 7 to Equation 8. The feed length is considered to be as double the guided quarter wavelength. Initially, substrate length and width are evaluated using Equation 9 which is considered approximately equal to three times the patch width (WP) and finally readjusted as per better results of resonance frequency, reflection coefficient, and -10dB fractional bandwidth (FBW). Similarly, at the initial stage, the ground length and width are considered the same as that of the RT Duroid 5880 substrate. The dimension of the reduced ground plane and inset cuts are obtained through the optometric function of ANSYS HFSS which is found to be 14.25 mm. The antenna geometry of the patch and moderate ground planes are shown in *Figures 2(a)* and *2 (b)*. The dimensional description of the designed antenna evaluated and simulated parameters are displayed in *Table 1*.

3.2.2Frequency selective surface design

Work on periodic surfaces was started in the mid-1960s because of the major military applications. However, the general principle was known long before. A patent is granted in 1919 to the famous Marconi and Franklin regarding the periodic structures. FSS is just a modified version of the periodic structure.

The proposed FSS works as a reflector for the back radiation and eventually, it suppresses the back lobe. Consequently, the front lobe level is increased in the forward direction and hence, the gain is increased. Therefore, the FSS serves as a reflector for the back lobes. The FSS has been designed on the single-

sided FR-4 substrate of the same size as that of the RT Duroid substrate. The FSS consists of 49 equally separated dipole elements. Each microstrip dipole has a length of 49 mm and a width of 0.25 mm. The spacing between the paralleled placed dipoles to each other is 1 mm. The dipole spacing (d), and dipole width (W_{dipole}) are optimized through the optometric in ANSYS HFSS software. The length of dipole (, the dipole length (L_{dipole}) strips is kept the same as that of the RT Duroid 5880 substrate. The working of FSS can be explained in terms of the dipole array excited by an incident wave. The co-polarization component of the back lobes excites current in the dipole array of the FSS which eventually radiates and contributes to the radiation from the particular patch antenna. The geometry of the frequency-selective surface beneath the moderate ground plane is illustrated in *Figure 3(a)*. The spacing between the reduced ground plane and FSS is obtained through the optometric which was found to be G=6.412 mm. The designed FSS with optimized dimensions is represented in *Figure 3(a)*. FSS consists of the series connection of equivalent inductors. The equivalent impedance Z_0 is the series combination of all the individual inductors of the dipole elements. The equivalent circuit of the FSS surface is displayed in *Figure 3(b)*. The final layout of the recommended antenna is shown in *Figure 4*. The dimensional description of the designed antenna parameters is displayed in *Table 1*.

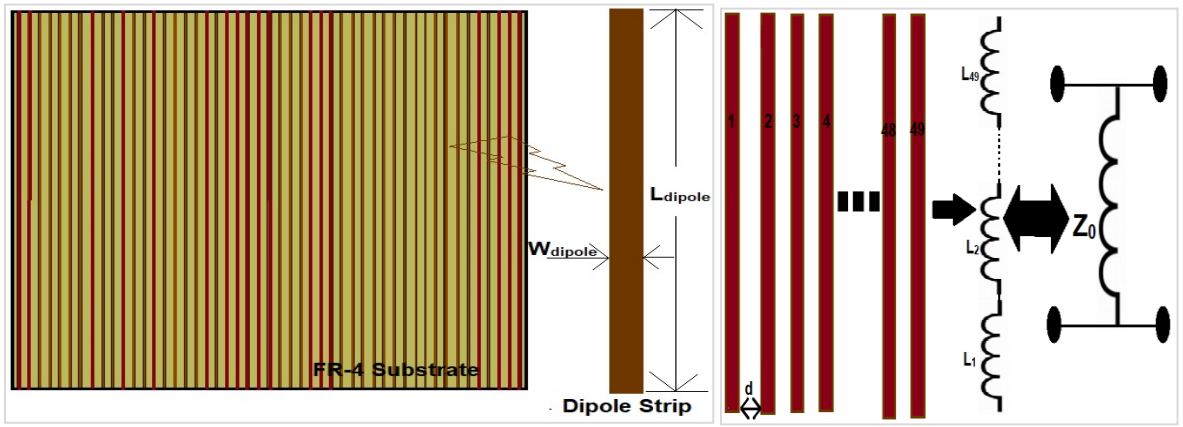

(a) (b)

Figure 3 Antenna reflector (a) FSS surface (dipole section) and (b) dipole strips and their equivalent

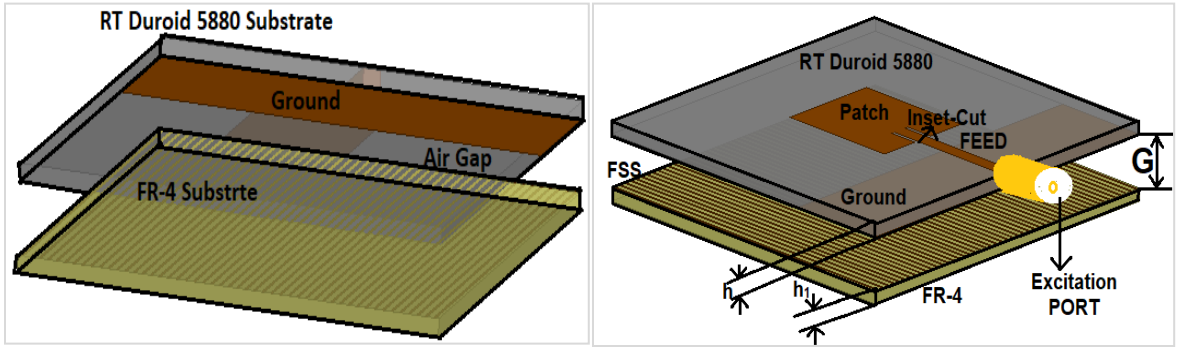

(a) (b)

Figure 4 Proposed patch antenna with FSS (a) bottom side view (b) trimetric view

3.3Electrical equivalent of the FSS antenna

The electrical equivalent of a microstrip rectangular patch antenna is represented as the parallel combination of R, L, and C values contributed by the patch and the ground plane due to existing substrate height and the permittivity as shown in *Figure 5(a)*. FSS is represented by an equivalent inductance contributed by the series combination of 49 rectangular dipole strips as displayed in *Figure 3(b)*. The FR-4 substrate is separated from the ground plane by an air gap thus this gap incorporated a parallel combination of an air capacitor and an air inductor.

Table 1 Proposed antenna design dimensions

Parameter name	Symbolic representation	Evaluated value (in mm)	Simulated or optimized value (in mm)
FR4 and RT Duroid 5880 Substrates width	$W_{sub}=L_{sub}$	44.12	49.0
FR4 and RT Duroid 5880 Substrates length	$L_{sub}=L_f+L_P+3h$	44.12	49.0
Patch width	W_P	16.493	14.25
Patch length	L_P	20.445	17.5
Microstrip feed width	W_f	3.986	2.0
Microstrip feed length	$L_f=\frac{\lambda g}{2}$	18.91	20
Inset-Cut width	W_i	0.5	0.5
Inset-Cut length	L_i	4.25	4.25
Ground width	W_{Gnd}	49.78	49.0
Ground length	L_{Gnd}	49	14.25
Height of RT Duroid 5880	h	1.588	1.588
Height of FR-4	$h_1=h$	1.588	1.588
The gap between two substrates	G	6.412	6.412
Width of dipole	W_{dipole}	0.25	0.25
Length of dipole	$L_{diopole}$	49.0	49.0
The separation between two dipoles	d	0.75	0.75
Number of dipoles	N	-----	49(Unit less)

This FSS effect is added in the equivalent circuit of the rectangular patch without FSS as displayed in *Figure 5(b).* The electrical equivalent circuit of the proposed antenna without FSS and with FSS is represented in *Figure 5* [7, 40]. FSS not only enhances the gain of the antenna but also provides the shifting in the resonance frequency.

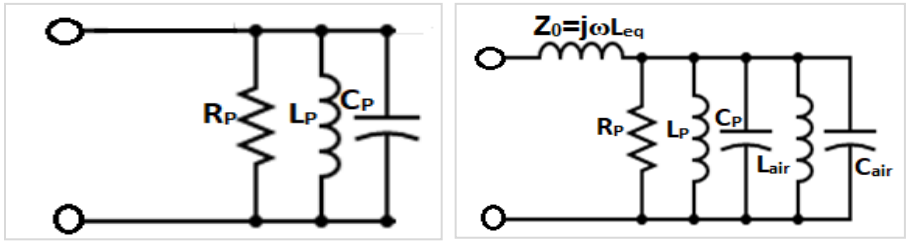

(a) (b)

Figure 5 Equivalent circuit of the patch antenna (a) without FSS and (b) with FSS

4.Results

4.1Parametric analysis

4.1.1Substrate Length (L_{Sub}) and Substrate Width (W_{Sub})

Initially, the design started with the standard substrate dimensions (26.021mm×44.12mm) evaluated using Equation 9 and Equation 10. In this case, all the reflection coefficient value is above -10dB and radiation efficiency is lower than 50%. Then the dimensions of the substrate width and length make equal 40.12mm. This again implies no reasonable resultant reflection coefficient value lower than -10dB. Further, the length and width are kept equal to twice the rectangular patch length ($2L_P$) i.e. 40.89mm this results in a -10dB narrow bandwidth from 6.58GHz to 6.80GHz with excellent radiation efficiency. Further to improve the reflection coefficient and -10dB BW the length and width are increased in equal proportionate to approximately 49.0 mm. This will results in wide bandwidth with enhanced gain and very good radiation efficiency as mentioned in *Table 2* and all five cases of substrate dimensions variations are depicted in *Figure 6.*

Table 2 Parametric of Substrate dimensions

Case/ Mode $W_{Sub}=L_{Sub}$ (mm)	Substrate Size $(W_{Sub}\times L_{Sub})mm^2$	f_r (GHz)	-10dBBand (f_L-f_H) (GHz)	Minimum S_{11} (dB)	-10dB FBW (%)	Gain (dBi)	Radiation efficiency η (%)
$W_{Sub}=3h+W_P+3h=26.021$	26.021×44.12	6.37	----	-7.31	----	4.03	49.96

$L_{Sub}= L_f+L_P+3h=44.12$							
$L_f+L_P+3h=44.12$	44.12×44.12	6.35	----	-8.47	----	5.29	98.92
$2L_P= 40.89$	40.89×40.89	6.69	6.58-6.80	-12.38	3.29	2.19	98.75
$3W_P=49.78$	49.78×49.78	4.04	----	-3.44	----	8.48	Invalid
49.0 (Proposed)	49.0×49.0	5.90	3.90-6.44	-19.23	49.13	7.63	97.36

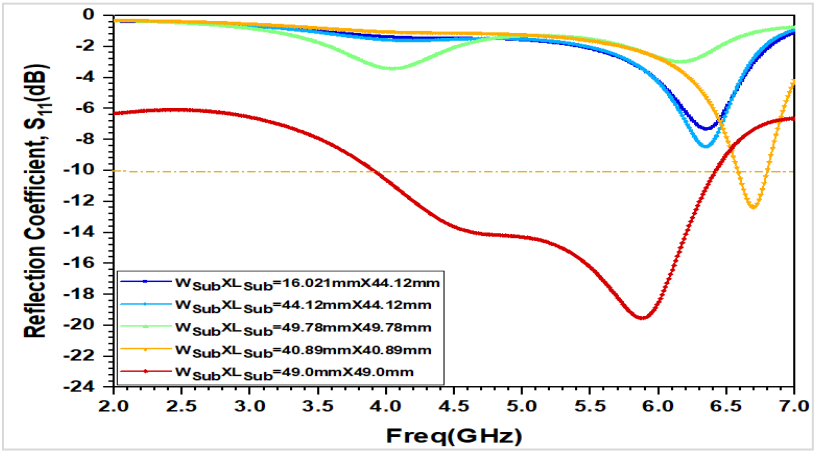

Figure 6 Parametric of substrate dimensions

4.1.2Patch width (W_P) and patch length (L_P)

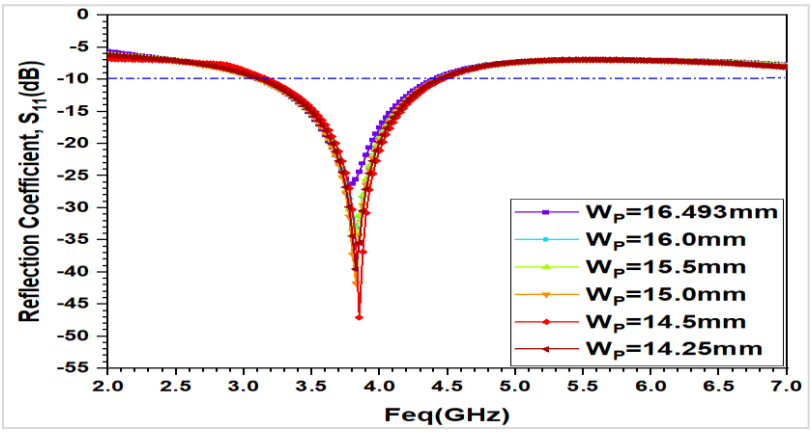

Figure 7 Parametric of rectangular patch width (W_P)

The rectangular patch width (W_P) is varied in a step size of 0.5mm by keeping the patch length (L_P) fixed to 20.445mm. It is noticed that the decreased value of W_P results in an improvement in the reflection coefficient (S_{11}) on the other hand it will result in decreased value of gain. The bandwidth and resonant frequency remain the same. All the parametric effects are arranged in *Table 3* and displayed in *Figure 7.* The rectangular patch length (L_P) is varied in a step size of 1.0mm by keeping the W_P fixed to 14.25mm. It is noticed that the decreased value of L_P results in the improvement in the -10dB FBW on the other hand it will shift the resonant frequencies towards the right and decrease reflection coefficient (S_{11}) while this results in the increased value of gain and radiation efficiency. All the parametric effects of patch length are arranged in *Table 4* and displayed in *Figure 8.*

Table 3 Parametric of rectangular patch width (W_P)

Case/ Mode W_P	Patch Size $(W_P \times L_P)mm^2$	f_r (GHz)	-10dBBand (f_L-f_H) (GHz)	Minimum S_{11} (dB)	-10dB FBW (%)	Gain (dBi)	Radiation efficiency η (%)
W_P	16.493×20.445	3.78	3.11-4.40	-26.23	34.35	4.10	97.19
W_P	16×20.445	3.83	3.14-4.43	-33.0	34.08	4.09	96.39
W_P	15.50×20.445	3.82	3.12-4.43	-33.78	34.70	3.93	96.97
W_P	15×20.445	3.83	3.11-4.44	-41.76	35.23	3.77	96.67
W_P	14.50×20.445	3.85	3.18-4.46	-47.06	33.50	3.83	97.41
W_P	14.25×20.445	3.83	3.12-4.443	-39.57	34.98	3.64	96.82

Table 4 Parametric of rectangular patch length (L_P)

Case/ Mode L_P (mm)	Patch Size $(W_P \times L_P)mm^2$	f_r (GHz)	-10dBBand (f_L-f_H) (GHz)	Minimum S_{11} (dB)	-10dB FBW (%)	Gain (dBi)	Radiation efficiency η (%)
L_P	14.25×20.445	3.83	3.12-4.443	-39.57	34.98	3.64	96.82
L_P	14.25×19.5	4.34	3.61-5.58	-22.94	42.87	8.41	93.07
L_P	14.25×18.5	4.59	3.75-6.03	-17.25	46.625	8.43	96.51
L_P	14.25×17.5	5.88	3.91-6.42	-19.53	48.59	7.70	97.88

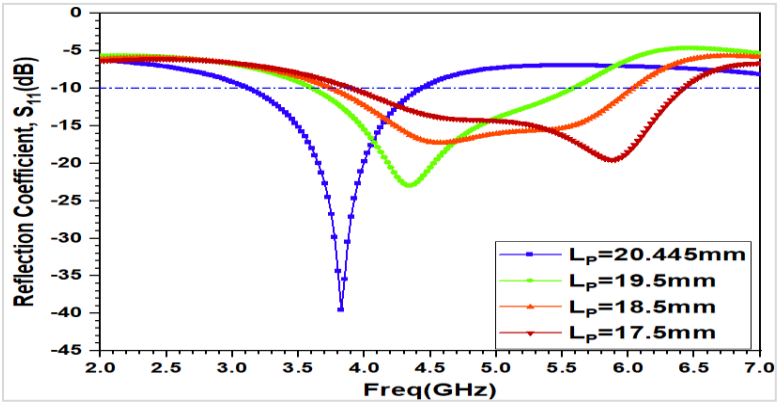

Figure 8 Parametric of rectangular patch length (L_P)

4.1.3Inset depth (L_i) and Inset Gap (W_i=0.5mm)

The Inset depth (L_i) is varied in a step size of 1mm by keeping the inset gap constant equal to 0.5mm. It is noticed that every time increase in depth (L_i) has shifted the resonance frequency towards right close to the design frequency 5.8GHz. It also improves the reflection coefficient more flatten and below -10dB. It also results in an enhanced value of gain. All variations of inset depth (Li) with fixed inset gap (W_i) are tabulated in *Table 5* and illustrated in *Figure 9*.

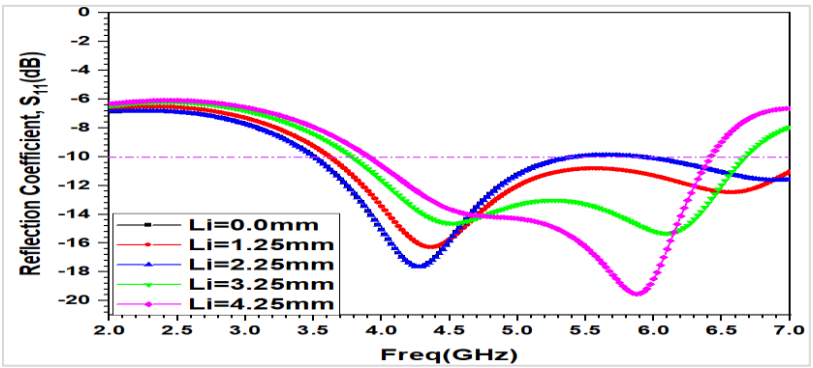

Figure 9 Parametric of inset-cut length (L_i)

Table 5 Parametric of inset depth length (L_i)

Case/ Mode L_i (mm)	f_r (GHz)	-10dBBand (f_L-f_H) (GHz)	Minimum S_{11} (dB)	-10dB FBW (%)	Gain (dBi)	Radiation efficiency η (%)
Li=0	4.29, 6.88	3.50-5.43, 5.90-7.50	-17.63, -11.62	43.225, 23.88	5.78	97.73
Li=1.25	4.37, 6.56	3.62-7.20	-16.27, -12.46	66.17	6.21	97.78
2.25	4.27, 6.89	3.50-5.43, 5.90-7.30	-17.64, -11.62	43.225, 21.55	5.75	97.73
3.25	4.50, 6.12	3.78-6.67	-14.63,-15.32	55.31	7.12	97.79
4.25	5.88	3.91-6.42	-19.53	48.59	7.70	97.88

4.1.4The gap between Two Substrates, G (Ground and FSS)

The adjustment of the gap between the two substrates' main patch and FSS layers, G in a step size of 1mm. Initially, the gap is kept at 5.12mm. To enhance the gain and widen the bandwidth with more flatness below -15dB of reflection coefficient S11, the gap is changed to 6.412mm and 7.412mm. In each parametric case the change in gap results in an excellent improvement in the gain value and FBW below -15dB as displayed in *Table 6* and represented in *Figure 10.*

Table 6 Parametric of Gap between two substrates, G (Ground and FSS)

Case/ Mode L_i (mm)	f_r (GHz)	-10dBBand (f_L-f_H) (GHz)	Minimum S_{11} (dB)	-10dB FBW (%)	Gain (dBi)	Radiation efficiency η (%)
5.412	5.97	4.13-6.47	-19.73		5.97	97.60
6.412	5.90	3.90-6.44	-19.23	49.13	7.63	97.36
7.412	5.80	3.74-6.40	-19.63		7.84	97.56

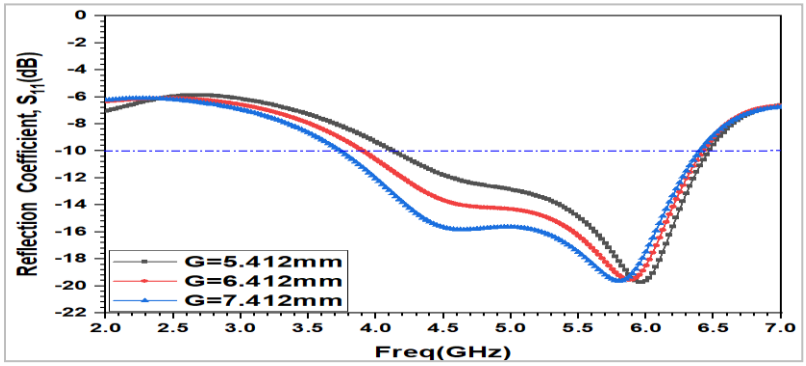

Figure 10 Parametric of Gap between two substrates (G)

4.1.5Separations between dipoles (d)

The end-to-end separation between the two dipoles of the FSS is changed with a step size of 0.25mm. Initially, the separation (d) is 0.50mm then in each parametric it will be increased to 0.75mm and then 1.0mm. It is observed that excellent radiation efficiency and the highest gain at a frequency of 5.8GHz is achieved. The parametric effect of the gap between the dipole is displayed in *Table 7* and indicated in *Figure 11.*

Table 7 Parametric of Gap between Two dipoles, d

Case/ Mode d (mm)	f_r (GHz)	-10dBBand (f_L-f_H) (GHz)	Minimum S_{11} (dB)	-10dB FBW (%)	Gain (dBi)	Radiation efficiency η (%)
0.50	5.90	3.91-6.42	-19.50	48.59	7.70	97.88
0.75	5.90	3.90-6.44	-19.23	49.13	7.63	97.36
1.0	5.97	4.13-6.47	-19.73	44.15	7.56	97.60

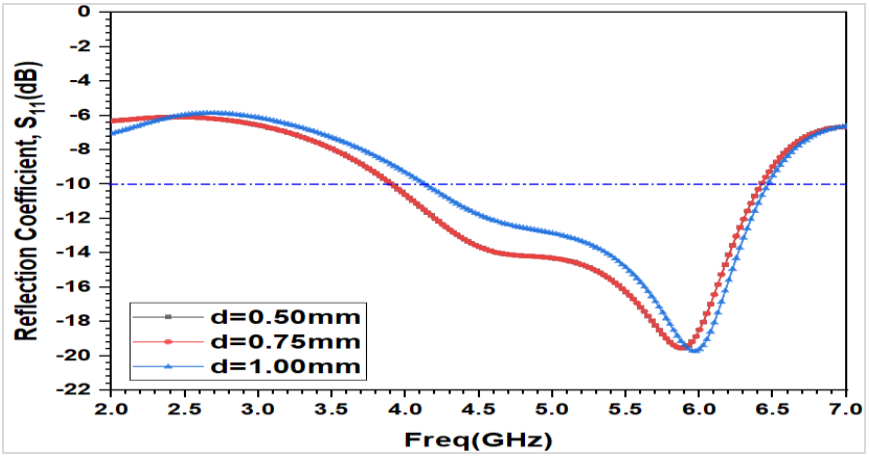

Figure 11 Parametric of gap between two dipoles (d**)**

4.1.6Effect of thickness of dipole (W_{dipole})

The thickness of the dipole is initially kept equal to 0.25mm. After that, the width of each dipole is increased with a step size of 0.25mm. Therefore, the width of each dipole becomes 0.50mm, 0.75mm, and 1.0mm. These parametric do not affect the reflection coefficient, FBW, and radiation efficiency. The parametric of the thickness of the dipole are arranged in *Table 8* and their reflection coefficients curve family is plotted in *Figure 12*

Table 8 Parametric of thickness of dipole (W_{dipole})

Case/ Mode W_{dipole} (mm)	f_r (GHz)	-10dBBand (f_L-f_H) (GHz)	Minimum S_{11} (dB)	-10dB FBW (%)	Gain (dBi)	Radiation efficiency η (%)
0.25	5.90	3.90-6.44	-19.23	49.13	7.63	97.36
0.50	5.90	3.91-6.38	-19.68	48.00	7.68	97.88
0.75	5.89	3.89-6.42	-19.54	49.08	7.76	96.87
1.0	5.86	3.80-6.41	-19.38	51.12	7.56	97.42

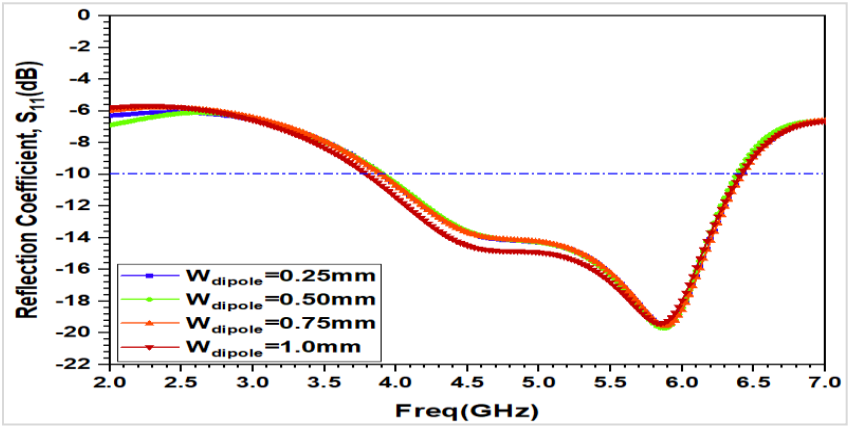

Figure 12 Parametric of thickness of dipole (W_{dipole})

4.2Effect of FSS as reflector on rectangular patch antenna

4.2.1Reflection Coefficient, S11, and voltage standing wave ratio(VSWR)

The plot of voltage standing wave ratio (VSWR) and reflection coefficients indicate a good impedance matching at the resonant frequency of 5.8 GHz. However, the -10 dB FBW is compromised a little for enhanced value of the gain. Without using of FSS -10dB FBW is more than 98% while it becomes down to 49% with the introduced FSS. The introduced FSS reduces the value of VSWR to 1.24

from 1.08 and enhances the gain by multi-fold from 2.87dBi to 7.70dBi at the cost of 50% reduced bandwidth. The reflection coefficient curves and VSWR plots of the antenna with and without FSS are represented in *Figure 13(a)* and *Figure 13(b)* respectively. It has been observed from the plots that S_{11} is decreased by positioning the FSS below the ground plane.

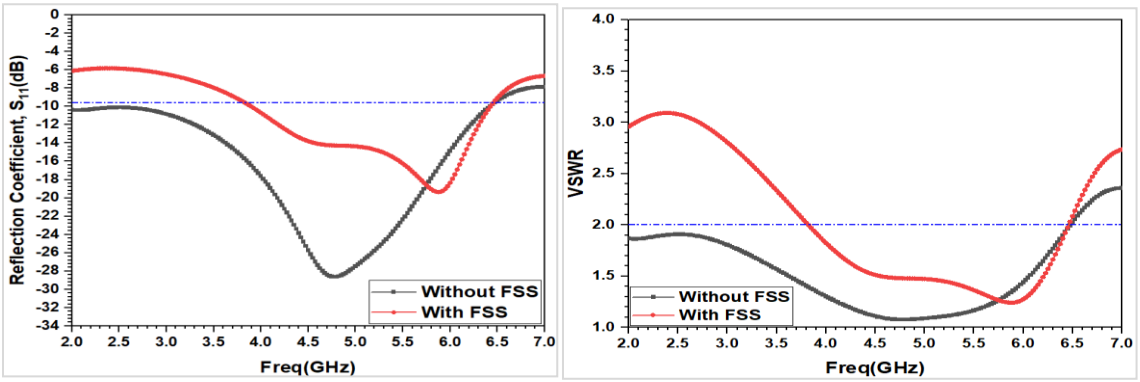

(a) (b)

Figure 13 (a) Reflection coefficients, S_{11} and (b) VSWR of the proposed antenna

4.2.2Gain and radiation efficiency

An antenna's gain indicates the strength of transmission power in the direction of maximum radiation concerning an isotropic source. In other words, it represents the antenna's magnitude in transmitting or receiving a signal in the specific path's direction. The simulated gain comparison of the antenna with FSS and without FSS is illustrated in *Figure 14(a)*. The lower black line plot represents the antenna gain without FSS while the upper red line plot represents the antenna gain after inclusion of the FSS reflector surface beneath the main antenna ground plane. The comparison indicates the observation of the gain vs frequency plots, the antenna gain with FSS is increased throughout the whole frequency range. It depicts an increase in the gain from 1dBi to 5dBi while at the resonant frequency of 5.8 GHz; the gain is enhanced from 2.72dBi to 7.76dBi. *Figure 14(b)* shows the comparison of the radiation efficiencies of the proposed antenna with FSS and without using the FSS. It is noticed from the graph in the resulting figure that the patch antenna with FSS has an efficiency of about 98% while the antenna without FSS efficiency is close to 94%. Therefore it is concluded that the FSS beneath the patch not only enhances the gain but also improves the radiation efficiency. All the resultant parameters without FSS and with FSS of the proposed structures are arranged in *Table 9.*

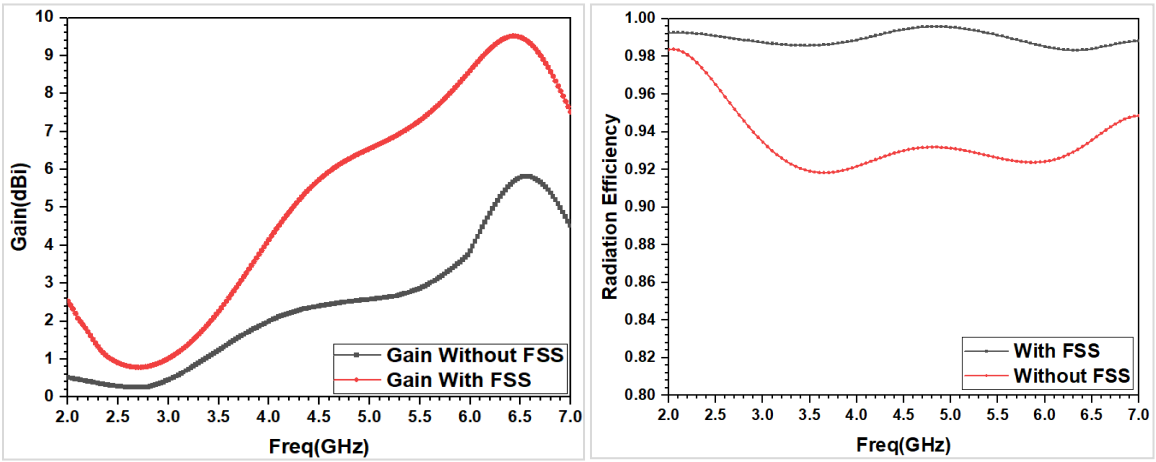

(a) (b)

Figure 14 (a) Gain Comparison (b) Comparison of the radiation efficiency

Table 9 Parametric of thickness of dipole (W_{dipole})

Case/ Mode	f_r (GHz)	-10dBBand (f_L-f_H) (GHz)	Minimum S_{11} (dB)	VSWR	-10dB FBW (%)	Gain (dBi)	Rad. Eff. η (%)
Without FSS	4.78	2.0-6.42	-28.64	1.08	98.12	2.87	94.68
With FSS	5.89	3.89-6.42	-19.54	1.24	49.08	7.76	97.88

4.2.3Radiation patterns

Antenna radiation pattern typically includes information about antenna directivity, antenna gain, half power beam width in E-plane and H-plane, FBR, etc. *Figure15 (a) Figure 15(b)* and *Figure 16(a), Figure 16(b)* indicate the comparison of the E_Φ and E_θ at Φ=0 plane and Φ=90 for the proposed antenna with FSS and without FSS. In the Φ=0 plane, the effect of FSS on EΦ is remarkable and the FSS is effectively reflecting the back radiation in the desired direction. On the other hand, the effect of FSS in the Φ=90 Plane is comparatively less pronounced. While in the case of the E_θ component, the effect of FSS can be observed in Φ=90 Plane. Its effect is negligible in the Φ=0 plane. *Figure 17(a), Figure 17(b)* illustrates the cross-polarisation levels at Φ=0 and Φ=90 axes. Polarization purity can be noticed in the Φ=0 plane along the bore sight direction while in Φ=90 it is having cross-polarization components. The FSS reflector consists of long parallel equidistant dipole strips with spacing <<λ0. The dipole strips were placed parallel to the larger size (length) of the patch antenna to improve the co-polarization level.

The 3D radiation patterns for the E_θ and E_Φ components without FSS and with FSS are shown in *Figures 18(a), Figure 18(b).* It is obvious from *Figure 17* that the FSS reflector reduces the level of back-radiated power and increases the level of power radiated in the forward direction. The FBR without using FSS is found to be 1.79 (2.53dB) while with FSS it is increased up to a value of 62.75 (approximately 18dB) which is a remarkable achievement.

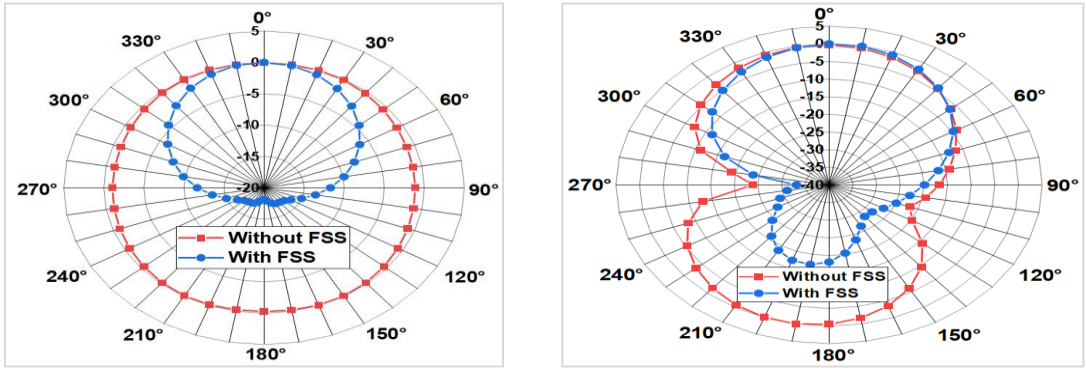

(a) (b)

Figure 15 Gain radiation patterns (a) at E_Φ in Φ=0 (E-Plane) (b) at E_Φ in Φ=90 (H-Plane)

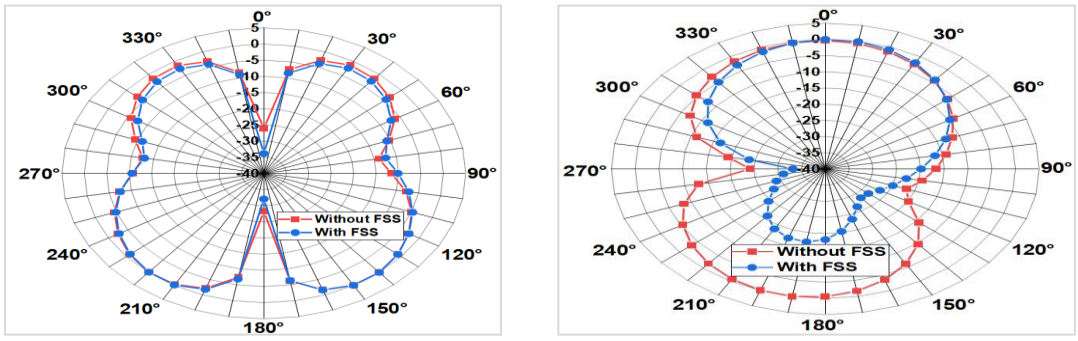

(a) (b)

Figure 16 Co-polarization (a) at E_θ in Φ=0 (E-Plane) (b) at E_θ in Φ=90 (H-Plane)

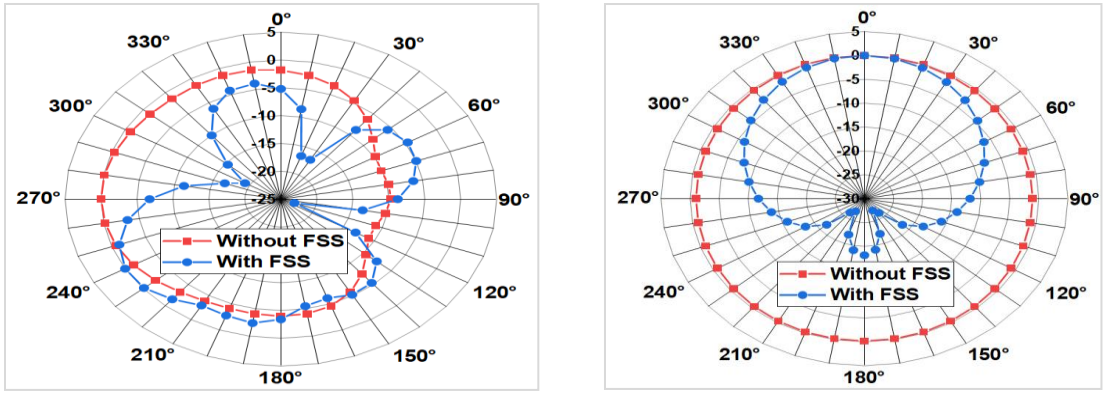

(a) (b)

Figure 17 Cross Polarization (a) at Φ=0 (E-Plane) (b) at Φ=90 (H-Plane)

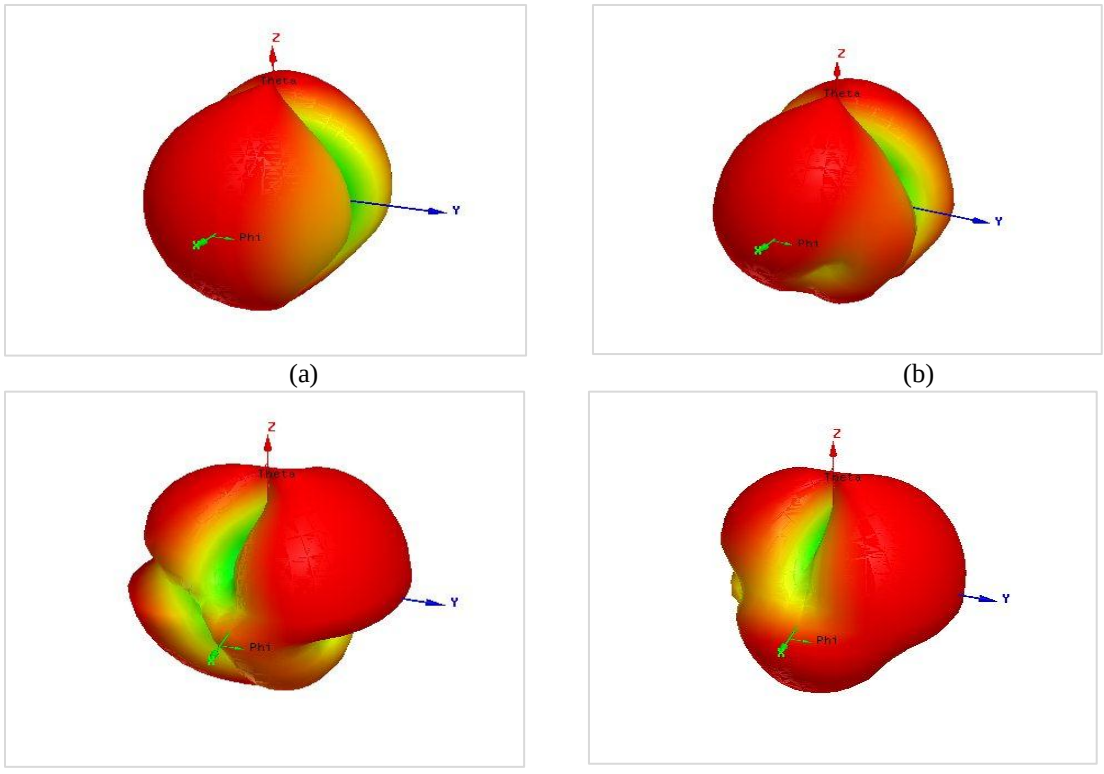

(a) (b)

(c) (d)

Figure 18 3D Radiation patterns (a) E_{Φ} without FSS (b) E_{Φ} with FSS (c) E_{θ} without FSS (d) E_{θ} with FSS

5. Discussions

In this study, the back lobes are reduced and an antenna's performance parameter is improved by locating FSS below the antenna acting as a reflector, as shown in *Figure 4.*

5.1 Comparison of the closely existing literature antennas

The resultant parameters of the proposed antenna with FSS 'show' that the antenna resonates at the designing frequency of 5.80GHz with a reflection coefficient of -19.54 dB. The gain after the integration of FSS is 7.76dBi, and the antenna radiation efficiency is also increased by an amount of 98.81%, which makes the antenna suitable for sub-6 GHz frequency applications. The resultant performance parameters comparison between the proposed antenna and the existing antenna models found in the literature are presented in *Table 10.* In the literature, the majority of antennas are made of

FR-4 substrate material. The comparisons table tells that the recommended antenna design has a maximum improvement of gain of 4.89dBi, which is significantly higher than the gains of the existing antennas. A comparison with existing similar antennas in the literature has been offered and shows that the present design is more compact, and the achieved radiation efficiency and gain are higher than the former works.

Table 10 Gain-enhancing comparison of the suggested antenna and published recently FSS/metasurface work

Ref. No.	Antenna Size (mm^3) (Antenna Type)	Design Freq., f_0 (GHz)	Method for Gain Enhancement	FBW f_L-f_H, (GHz)	Rad. Eff., η (%)	Gain (dBi)	Gain enhancement (dBi)
Varshney et al. [7], 2022	66.4×66.4 × 1.6 FR-4 (Monopole)	2.45	SRR triplet (without reflector)	1.81-3.0	92.85	7.16	7.286 to 7.16
Nakmouche et al. [18], 2021	50× 50 × 1.6 RT Duroid 5880 (Monopole)	6.0	FSS	5.53-6.36	>95	8.89	3.12 to 8.89
Ghosh et al. [29], 2016	60 × 60 × 1.6 FR4	3.75, 5.98 and 8.79 (Multi-band)	AMC (Double Layer)	Multi-band, 3.75, 5.98 and 8.79		7.52	3.88 to 4.93
Belen et al. [32], 2020	50 × 53.4 × 1.6 FR4	2.4	DRA-FSS	2.4	NA	8.6	3 to 8.6
Bhattacharya et al. [34], 2021	40 × 30 × 0.8 (DR height = 4.3 mm)	8.15–13.2 (5.05)	FSS (Double side)	8.15–13.2 (5.05)	NA	7.8	3.3 to 7.8
Hussain et al. [35], 2023	32 × 25 × 1.52 Rogers RT/Duroid 6002	12.0	FSS	5-18	>90	10.5	6.5-10.5
Belen [37], 2018	63.65 × 54.16 × 1.588	2.4	Band-Pass FSS (Double Layer)	2.4	NA	7	5 to 7
Patel and Raval [41], 2021	60× 50 × 1.6 (FR-4)	5.8	SIW Cavity Backed antenna using dielectric loading, FR4 cylinder, Teflon cylinder	5.7-5.9	NA	8.13	3.13 to 8.13
Belabbas et al. [42], 2021	20× 20 × 1.6 RT Duroid TTN	28.4	Asymmetric AMC ground plane (Impedance surface)	28.4-36	NA	8.30	4 to 8.3
Jing et al. [43], 2023	50.4× 28 × 0.1 Polyimide (PI) substrate	2.4	3×3 rotatable curved FSS	2.18-2.90	NA	8.31	3 to 8.31
Proposed	49 x49 x1.588 RT Duroid 5880 and FR4 (Monopole)	5.8	FSS as a reflector (Double Layer)	3.91-6.44	97.88	7.76	2.87 o 7.76

5.2 Limitation

The proposed antenna has wide bandwidth, high gain, and very high radiation efficiency values even though it has several limitations. As the FSS surface is arranged beneath the ground at some gap, increases the antenna size in the third dimension and hence will occupy more space. Since the main rectangular patch antenna is designed on the RT Duroid 5880, this will make the antenna costly. FSS improves the gain and radiation efficiency but reduced reflection coefficient. As the antenna has wide-bandwidth from 3.91GHz to 6.44GHz it is suitable to sub-6 GHz applications like n46 (5150 – 5925MHz), n47 (5855 – 5925MHz), n77 (3900-4200MHz), n79 (4400-5000MHz), n96/n102 (5925-6425MHz) bands. The numbers of 5G sub-6 GHz applications like the n78 band and others can be improved by increasing the antenna patch length to 20.445mm instead of 17.5mm. In most of the work same substrate material was used for the radiator as well as the FSS structure, and complex geometries were fabricated, those are difficult to manufacture. In the present study different substrates are used for both radiators as well as the FSS design and simple strip lines were used for the construction of the FSS.

A complete list of abbreviations is shown in *Appendix I.*

6. Conclusion and future work

A modern technique based on FSS was presented in this paper to enhance the gain and efficiency of a microstrip antenna. The FSS reflector consists of long, parallel, equidistant dipole strips with spacing much smaller than the wavelength (<<λ0). To increase the co-polarization level, the dipole strips are positioned parallel to the longer dimension (patch length) of the patch antenna. Simulation results show a remarkable enhancement in the antenna's gain, from 1 dBi to 6 dBi, and efficiency, from 92% to 99%, by using this FSS as a reflector for the main patch antenna. These results indicate that the FSS reflector effectively reflects the back lobes in the desired direction without introducing cross-polarization. The simulation results were optimized using the built-in optimization tool of the ANSYS HFSS software. The proposed antenna is most suitable for sub-6 GHz applications. In the future, the antenna could be reconfigured for other frequency bands such as n78, etc., by increasing the patch length to about 3mm and connecting a PIN diode while keeping the patch width and other parameters constant. Further gain enhancement could be achieved by replacing the array of rectangular strips with an array of SRRs, EBG structures, RIS, or other advanced technologies like fractal and DRA, slotted sections, and hybridization.

Acknowledgment

The authors would like to express their sincere thanks to the director, my supervisor and supporting staff of the School of Engineering & Technology, University of Petroleum & Energy Studies, Dehradun (Uttarakhand) for providing the research environment and support in conducting the research. The authors would also say thanks to the editors and reviewers whose input and recommendations contributed to improving the manuscript's quality.

Conflicts of interest

The authors have no conflicts of interest to declare.

Author's contribution statement

Shabnam Ara: Conceptualization, investigation, writing – original draft, writing – review and editing. **Dr. Prasanthi Kumari Nunna: S**tudy conception, design, supervision, investigation on challenges and draft manuscript preparation.

References

[1] Li LW, Li YN, Yeo TS, Mosig JR, Martin OJ. A broadband and high-gain metamaterial microstrip antenna. Applied Physics Letters. 2010; 96(16).

[2] Devarapalli AB, Moyra T. Design of a metamaterial loaded W-shaped patch antenna with FSS for improved bandwidth and gain. Silicon. 2023; 15(4):2011-24.

[3] Varshney A, Sharma V, Neebha TM, Kumar R. A compact low-cost impedance transformer-fed wideband monopole antenna for Wi-MAX N78-band and wireless applications. Printed Antennas: Design and Challenges. 2022.

[4] Yuan Y, Xi X, Zhao Y. Compact UWB FSS reflector for antenna gain enhancement. IET Microwaves, Antennas & Propagation. 2019; 13(10):1749-55.

[5] Al-gburi AJ, Ibrahim IB, Zeain MY, Zakaria Z. Compact size and high gain of CPW-fed UWB strawberry artistic shaped printed monopole antennas using FSS single layer reflector. IEEE Access. 2020; 8:92697-707.

[6] Asimakis NP, Karanasiou I, Uzunoglu N. Non-invasive microwave radiometric system for intracranial applications: a study using the conformal L-notch microstrip patch antenna. Progress in Electromagnetics Research. 2011; 117:83-101.

[7] Varshney A, Cholake N, Sharma V. Low-cost ELC-UWB fan-shaped antenna using parasitic SRR triplet for ISM band and PCS applications. International Journal of Electronics Letters. 2022; 10(4):391-402.

[8] Nakmouche MF, Allam AM, Fawzy DE, Lin DB. Low profile dual band H-slotted DGS based antenna design using ANN for K/Ku band applications. In 2021 8th international conference on electrical and electronics engineering 2021 (pp. 283-6). IEEE.

[9] Nakmouche MF, Taher H, Fawzy DE, Allam AM. Development of a wideband substrate integrated waveguide bandpass filter using H-slotted DGS. In IEEE conference on antenna measurements & applications 2019 (pp. 1-4). IEEE.

[10] Ara S, Nunna PK. ASIM shape wide band high-gain patch antenna integrated with frequency-selective surface as super strate for sub-6GHz5G applications. International Journal on Recent and Innovation Trends in Computing and Communication. 2022; 10(2s):23-8.

[11] Kapoor A, Mishra R, Kumar P. Frequency selective surfaces as spatial filters: Fundamentals, analysis and applications. Alexandria Engineering Journal. 2022; 61(6):4263-93.

[12] Ara S, Nunna PK. High gain, compact design integrated with FSS as superstrate in patch antenna for Sub6 Ghz 5G application. In international conference on device intelligence, computing and communication technologies 2023 (pp. 80-5). IEEE.

[13] Marhoon HM, Qasem N, Basil N, Ibrahim AR. Design and simulation of a compact metal-graphene frequency reconfigurable microstrip patch antenna with FSS superstrate for 5G applications. International Journal on Engineering Applications. 2022; 10(3):193-201.

[14] Raj A, Gupta N. Radiation characteristics of microstrip antenna on frequency selective surface absorbing layer. International Journal of Microwave and Wireless Technologies. 2021; 13(9):962-8.

[15] Patil SM, Rajeshkumar V. Metamaterial based triple-band circular patch antenna for 5G Sub 6 GHz

applications. In wireless antenna and microwave symposium 2022 (pp. 1-4). IEEE.
[16] Olawoye TO, Kumar P. A high gain antenna with DGS for sub-6 GHz 5G communications. Advanced Electromagnetics. 2022; 11(1):41-50.
[17] Nakmouche MF, Nassim M. Impact of metamaterials DGS in PIFA antennas for IoT terminals design. In 6th international conference on image and signal processing and their applications 2019 (pp. 1-4). IEEE.
[18] Nakmouche MF, Allam AM, Fawzy DE, Lin DB. Development of a high gain FSS reflector backed monopole antenna using machine learning for 5G applications. Progress in Electromagnetics Research M. 2021; 105:183-94.
[19] Raveendra M, Saravanakumar U, Kumar GA, Suresh P, Pedapalli SP. A multiband substrate integrated waveguide antenna for Ku-band and K-band applications. In 6th international conference for convergence in technology 2021 (pp. 1-4). IEEE.
[20] Munk BA. Frequency selective surfaces: theory and design. John Wiley & Sons; 2005.
[21] Güneş F, Belen MA, Mahouti P. Performance enhancement of a microstrip patch antenna using substrate integrated waveguide frequency selective surface for ISM band applications. Microwave and Optical Technology Letters. 2018; 60(5):1160-4.
[22] Vardaxoglou JC. Frequency selective surfaces: analysis and design. Research Studies Press Wiley; 1997.
[23] Kim JH, Ahn CH, Bang JK. Antenna gain enhancement using a holey superstrate. IEEE Transactions on Antennas and Propagation. 2016; 64(3):1164-7.
[24] Sarkhel A, Bhadra CSR. Enhanced-gain printed slot antenna using an electric metasurface superstrate. Applied Physics A. 2016; 122:1-11.
[25] Fernandes EM, Da SMW, Da SBL, De SCAL, De AHX, Casella IR, et al. 2.4–5.8 GHz dual-band patch antenna with FSS reflector for radiation parameters enhancement. AEU-International Journal of Electronics and Communications. 2019; 108:235-41.
[26] Tilak GB, Kotamraju SK, Madhav BT, Kavya KC, Rao MV. Dual sensed high gain heart shaped monopole antenna with planar artificial magnetic conductor. Journal of Engineering Science and Technology. 2020; 15(3):1952-71.
[27] Zhai H, Zhang K, Yang S, Feng D. A low-profile dual-band dual-polarized antenna with an AMC surface for WLAN applications. IEEE Antennas and Wireless Propagation Letters. 2017; 16:2692-5.
[28] Liu Q, Liu H, He W, He S. A low-profile dual-band dual-polarized antenna with an AMC reflector for 5G communications. IEEE Access. 2020; 8:24072-80.
[29] Ghosh A, Mandal T, Das S. Design of triple band slot-patch antenna with improved gain using triple band artificial magnetic conductor. Radioengineering. 2016; 25(3).442-8.
[30] Chatterjee A, Parui SK. Gain enhancement of a wide slot antenna using a second-order bandpass frequency selective surface. Radioengineering. 2015; 24(2):455-61.
[31] Gharsallah H, Osman L, Latrach L. Circularly polarized two-layer conical DRA based on metamaterial. Microwave and Optical Technology Letters. 2017; 59(8):1913-9.
[32] Belen MA, Mahouti P, Palandöken M. Design and realization of novel frequency selective surface loaded dielectric resonator antenna via 3D printing technology. Microwave and Optical Technology Letters. 2020; 62(5):2004-13.
[33] Ram KRV, Kumar R. Slotted ground microstrip antenna with FSS reflector for high-gain horizontal polarisation. Electronics Letters. 2015; 51(8):599-600.
[34] Bhattacharya A, Dasgupta B, Jyoti R. Design and analysis of ultrathin X-band frequency selective surface structure for gain enhancement of hybrid antenna. International Journal of RF and Microwave Computer-Aided Engineering. 2021; 31(2).
[35] Hussain M, Sufian MA, Alzaidi MS, Naqvi SI, Hussain N, Elkamchouchi DH, et al. Bandwidth and gain enhancement of a CPW antenna using frequency selective surface for UWB applications. Micromachines. 2023; 14(3):1-13.
[36] Ranga Y, Matekovits L, Esselle KP, Weily AR. Multioctave frequency selective surface reflector for ultrawideband antennas. IEEE Antennas and Wireless Propagation Letters. 2011; 10:219-22.
[37] Belen MA. Performance enhancement of a microstrip patch antenna using dual-layer frequency-selective surface for ISM band applications. Microwave and Optical Technology Letters. 2018; 60(11):2730-4.
[38] Ali M, Arya RK, Yerrola AK, Murmu L, Kumar A. Bandwidth and gain enhancement with cross-polarization suppression in microstrip antenna with superstate. In XXXIVth general assembly and scientific symposium of the international union of radio science 2021 (pp. 1-4). IEEE.
[39] Chang K. RF and microwave wireless systems. John Wiley & Sons; 2004.
[40] Balanis CA. Antenna theory: analysis and design. John Wiley & Sons; 2012.
[41] Patel DM, Raval F. Gain enhancement of SIW cavity-backed antenna using dielectric loading. Progress in Electromagnetics Research C. 2021; 111:61-72.
[42] Belabbas K, Khedrouche D, Hocini A. Artificial magnetic conductor-based millimeter wave microstrip patch antenna for gain enhancement. Journal of Telecommunications and Information Technology. 2021(1):56-63.
[43] Jing H, He G, Wang S. Design of a flexible cylindrical antenna with rotatable curved frequency selective surface for omnidirectional high-gain applications. International Journal of Antennas and Propagation. 2023; 2023:1-15.

Shabnam Ara was born in U.P., India. She earned her B.Tech degree from G.E.I.T (H.N.B. University) in 2008 and her M.Tech degree from Graphic Ere University in 2014. Currently, she is pursuing a Ph.D. at the University of Petroleum and Energy Studies, Dehradun. Since March 2019, she has been serving as an Assistant Professor in the Electronics and Communication Engineering Department at Shivalik College of Engineering in Dehradun. With a total of 12 years of work experience, she has a background in both industry and academics.

Email: shabnam.ara3012@gmail.com

Dr. Prasanthi Kumari Nunna was born in A.P, India. She received her B.Tech degree in Electronics and Communication Engineering from J.N.T.U. (Campus, Kakinada), an M.Tech. in Digital Systems, Computer, and Electronics from J.N.T.U. (Campus, Ananthapur), and a Ph.D. in Electronics from the University of Petroleum and Energy Studies, Dehradun, in 2015. Since 2009, Dr. Prasanthi Kumari Nunna has been working as an associate professor at the University of Petroleum and Energy Studies in Dehradun. Her areas of expertise include antenna design, low-power VLSI circuits, RF circuits, and metamaterials and their applications. With a total of 20 years of experience in academics, she has established herself as an expert in her field.

Email: prasanti@ddn.upes.ac.in

Appendix I

S. No.	Abbreviation	Description
1	3D	Three Dimensional
2	5 G	Fifth Generation
3	AMC	Artificial Magnetic Conductor
4	CPW	Coplanar Wave Guide
5	DGS	Defective Ground Surface
6	DRA	Dielectric Resonator Antenna
7	EBG	Electromagnetic Band Gap
8	FBR	Front-to-Back Ratio
9	FBW	Fractional Bandwidth
10	FR-4	Flame Retardant-4
11	FSS	Frequency Selective Surface
12	HFSS	High-Frequency Structure Simulator
13	ISM	Industrial Scientific and Medical
14	MPA	Microstrip Patch Antenna
15	PIFA	Planar Inverted-F Antenna
16	RIS	Resistive Interface Surface
17	RLC	Resistive Inductive Capacitive
18	SIW	Substrate Integrated Waveguide
19	SFS	Stepless Frequency Selection
20	SRR	Split Ring Resonator
21	UWB	Ultra-Wideband
22	VSWR	Voltage Standing Wave Ratio
23	WLAN	Wireless Local Area Network
24	W_P	Patch Width